Cell, Vol. 117, 29–45, April 2, 2004, Copyright ©2004 by Cell Press

Crossover/Noncrossover Differentiation, Synaptonemal Complex Formation, and Regulatory Surveillance at the Leptotene/Zygotene Transition of Meiosis

G. Valentin Börner,[1] Nancy Kleckner,[1,*] and Neil Hunter[1,2]

[1]Department of Molecular and Cellular Biology
Harvard University
Cambridge, Massachusetts 02138

[2]Center for Genetics and Development
Section of Microbiology
University of California
Davis, California 95616

Summary

Yeast mutants lacking meiotic proteins Zip1, Zip2, Zip3, Mer3, and/or Msh5 (ZMMs) were analyzed for recombination, synaptonemal complex (SC), and meiotic progression. At 33°C, recombination-initiating double-strand breaks (DSBs) and noncrossover products (NCRs) form normally while formation of single-end invasion strand exchange intermediates (SEIs), double Holliday junctions, crossover products (CRs), and SC are coordinately defective. Thus, during wild-type meiosis, recombinational interactions are differentiated into CR and NCR types very early, prior to onset of stable strand exchange and independent of SC. By implication, crossover interference does not require SC formation. We suggest that SC formation may require interference. Subsequently, CR-designated DSBs undergo a tightly coupled, ZMM-promoted transition that yields SEI-containing recombination complexes embedded in patches of SC. *zmm* mutant phenotypes differ strikingly at 33°C and 23°C, implicating higher temperature as a positive effector of recombination and identifying a checkpoint that monitors local CR-specific events, not SC formation, at late leptotene.

Introduction

Segregation of homologous chromosomes (homologs) at the first division of meiosis (MI) requires that they be physically connected. In most organisms, these connections occur at discrete points called chiasmata, where homologs have reciprocally exchanged chromosome arms to form a crossover (CR; Figures 1A and 1B). Crossovers comprise exchange both between the DNA/chromatin and between the underlying structural axes of the two involved chromatids (Figure 1 of Blat et al., 2002).

A particularly interesting feature of CRs is that their distribution is highly regulated. This distribution is characterized by two basic features (e.g., Figure 1B; Jones, 1984). First, every pair of homologs acquires at least one CR, despite the fact that the average number of CRs per chromosome is usually just one or a few. Second, the presence of a CR at one position is accompanied by a decreased probability that another will occur nearby. This latter property, known as CR or chiasma interference, has the overall effect that multiple CRs tend to be relatively evenly spaced. Nonrandom CR distribution is particularly intriguing because CRs do not occur at fixed positions in every meiotic nucleus. Thus, a highly specified pattern is arising without unique positional specification guided by underlying genetic determinants. Meiotic chiasmata may not be the only chromosomal features that exhibit these types of patterns and may therefore serve as a general model for spatial patterning of events along chromosomes (Kleckner et al., 2004).

The final distribution of meiotic CRs arises from a much larger number of precursor interactions by the regulated bifurcation of the recombination pathway (Figure 1C). At the DNA level, a large number of recombinational interactions are initiated via programmed double-strand breaks (DSBs; Keeney, 2001; Lichten, 2001). Then, at some key decision point, a subset of interactions is designated to mature specifically as interhomolog CRs, with the appropriate distribution. The remaining DSBs are also processed via interaction with the homolog but these interactions are resolved without accompanying exchange of chromosome arms, primarily as noncrossovers (NCRs; Figure 1C).

Neither the timing nor the mechanism of this crossover control process has been defined. Darlington proposed that crossovers arose around the time that chiasmata appear, i.e., at diplotene, via a torsional process related to metaphase chromosome coiling (Darlington, 1937); however, cytological studies later identified CR-correlated recombination nodules that appeared along the chromosomes at pachytene, implying an earlier designation point (von Wettstein et al., 1984; Carpenter, 1987). Elucidation of the structure of DNA provoked the classical Holliday model for recombination, which implied that CR/NCR differentiation occurred at the end of the process, with alternate resolution of Holliday junctions directly yielding CR and NCR products (Holliday, 1964). This feature was retained in later models.

Specific information regarding the timing of crossover control has been provided by physical studies of yeast recombination. This approach has defined a multistep progression of DNA events that occupies essentially all of meiotic prophase. DSB formation is followed by the sequential appearance of two prominent strand exchange intermediates, single-end invasions (SEIs) and double Holliday junctions (dHJs), which represent, respectively, the outcome of strand exchange first at one DSB end and then at the other (for discussion see Hunter and Kleckner, 2001; Schwacha and Kleckner, 1995). DSBs, SEIs, and dHJs are all long-lived species, thus implying the existence of four successive discrete transitions: DSB formation, onset of SEI formation, onset of dHJ formation, and onset of dHJ resolution into products (Figure 1E). Each transition occurs in temporal coordination with the basic cytological stages of meiotic prophase (Hunter and Kleckner, 2001). These stages are conveniently defined by the status of the synaptonemal complex (SC), a highly conserved structure that connects the axes of homologs, along their entire lengths,

*Correspondence: kleckner@fas.harvard.edu

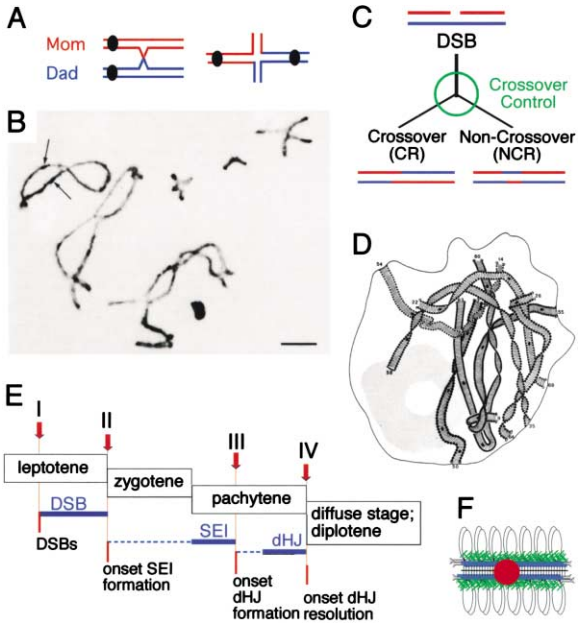

Figure 1. Features of Meiosis

(A) Reciprocal exchange between one sister chromatid of each homolog (Mom and Dad), plus connections between sister chromatids along their arms, creates a chiasma.

(B) Diplotene nucleus of grasshopper *Chorthippus bruneus* showing homologs linked by chiasmata (Jones, 1984).

(C) Meiotic recombination is initiated via programmed DSBs and yields both CRs and NCRs due to regulated bifurcation, e.g., after DSBs.

(D) 3D reconstruction of *Sordaria macrospora* pachytene nucleus showing paths of 7 SCs corresponding to 7 homolog pairs (Zickler, 1977).

(E) Four discrete DNA transitions of meiotic recombination, defined by physical studies in yeast (see also Figure 2A), occur at specific times in relation to global chromosome stages defined by SC status (Hunter and Kleckner, 2001). At leptotene, SC is absent; at zygotene, SC is forming; at pachytene, SC is full length (e.g., Panel D).

(F) At pachytene, SC links axes of homologs at ~100 nm. Chromatin loops of homologs emanate outward from edges of the structure, which are formed by the two homolog structural axes. Sites of CRs are marked by cytologically prominent SC-associated structures, "late recombination nodules," seen by electron microscopy, and correlated immunostaining foci.

at a distance of ~100 nm via a close-packed array of transverse filaments (e.g., Figure 1D). DSBs occur prior to appearance of any SC (leptotene); onset of SEI formation is concomitant with onset of SC formation (late leptotene/early zygotene) and SEI formation is completed during the period of SC formation (zygotene); onset of dHJ formation occurs during the period when SC is present (pachytene); and resolution of dHJs occurs at the end of pachytene (Figure 1E). CR and NCR products both appear at about this same time (Storlazzi et al., 1995; for discussion see Hunter and Kleckner, 2001; M. Lichten, personal communication; below).

All available evidence suggests that crossover control is imposed during or prior to formation of SEIs and SCs, i.e., during or prior to zygotene. Cytological features that are specifically correlated with CRs versus NCRs, e.g., SC-associated, CR-correlated "recombination nodules" (Figure 1F), appear as early as zygotene, well before the appearance of dHJs at mid-pachytene or resolution of dHJs at the end of pachytene (revewed by Zickler and Kleckner, 1999). This finding led to the suggestion that crossover control might be imposed at the DSB stage (Storlazzi et al., 1996). Subsequent studies have shown that the long-lived dHJs seen during wild-type meiosis are precursors specifically of CRs (Allers and Lichten, 2001) and that crossover control occurs concomitant with or prior to formation of SEIs (Hunter and Kleckner, 2001). The latter study further suggested that crossover control might be imposed at a point where DSBs are already engaged in nascent, undetected interactions with their homolog, but have not yet undergone stable strand exchange to give detectable SEIs.

Another unsolved problem with respect to crossover control in particular, and with respect to meiotic recombination in general, is the role of the SC. At the pachytene stage, sites of (future) CRs are marked by SC-associated "nodules" or "bars," seen in ultrastructural studies of several organisms (Figure 1F; reviewed by Zickler and Kleckner, 1999) and by correlated immunostaining foci of relevant proteins (Moens et al., 2002). Early models proposed that the SC might either play a "supporting structural role" and/or that SC polymerization might mediate crossover interference (Egel, 1978), a possibility also favored in more recent considerations (Sym and Roeder, 1994). On the other hand, it has also been proposed that crossover control occurs prior to and independent of SC formation (Storlazzi et al., 1996).

The relationship between recombination and the SC also has a second face: what is the role of recombination for SC formation? In fungi, mammals, and plants, mutations that affect proteins involved directly in recombination also abrogate SC formation, pointing to dependence of SC formation upon recombination (for discussion see Zickler and Kleckner, 1999; for yeast, see Alani et al., 1990). Also, in several such organisms, SC formation is nucleated specifically or preferentially at sites that ultimately become CRs or chiasmata, suggesting a local dependency or interdependency between crossover site designation and SC nucleation (Maguire, 1966; review in Zickler and Kleckner, 1998). However, in certain invertebrates (e.g., *Drosophila*, *C. elegans*, and female *Bombyx*), SC can form in the absence of recombination; the basis for this unique behavior also remains to be determined (discussion in Hunter, 2003; below).

A further important feature of meiotic prophase is checkpoint surveillance. In yeast, mutations that abrogate recombination at post-DSB stages also confer arrest or delay in progression out of prophase, presumably due to the operation of regulatory surveillance mechanisms (Bishop et al., 1992; Lydall et al., 1996; reviewed in Roeder and Bailis, 2000). It has been unclear whether these mechanisms are monitoring local events of recombination and/or SC formation, primarily because all relevant mutations affect both processes. It is also controversial whether these mechanisms are monitoring defects at late leptotene/zygotene and/or pachytene.

The current study further addresses all of the above issues. We have analyzed the effects of mutations in five meiosis-specific genes in yeast. Two of the corresponding proteins are presumed to be involved directly in the DNA biochemistry of meiotic recombination: Mer3, a DNA helicase and Msh5, a MutS homolog that acts with Msh4 and is not involved in mismatch repair. A third

is the structural protein Zip1, which ultimately comprises the central region of the SC (Nakagawa and Ogawa, 1999; Hollingsworth et al., 1995; Novak et al., 2001; Sym et al., 1993). The remaining two proteins are Zip2 and Zip3, whose molecular functions are unknown (Chua and Roeder, 1998; Agarwal and Roeder, 2000). Previous studies have shown that, in each case, absence of the protein confers defects in recombination, SC formation, and meiotic progression. These and other studies suggested more specifically that total levels of recombination initiation and interhomolog bias were robust, leading to high levels of "heteroallelic recombination" while CR levels were reduced and, at least in some cases, NCR levels were increased (Engebrecht et al., 1990; Storlazzi et al., 1995). Despite these similarities, however, mutant phenotypes differ substantially, and moreover, the phenotype of a single mutation differs depending on the strain background and/or experimental conditions used. These complications have confounded attempts to clearly define the roles of these ZMM proteins. We have therefore examined recombination, SC formation, and meiotic progression in a single isogenic set of wild-type and mutant strains. A key component of our analysis was examination of these processes, in parallel, at 33°C and 23°C instead of 30°C, the standard temperature for yeast studies.

All mutants and mutant combinations exhibit a shared common phenotype, implying that these "ZMM" proteins work coordinately. Details of mutant phenotypes and differences between mutant phenotypes at 23°C and 33°C provide new information about all of the assayed processes and their relationships and implicate temperature as an important variable for meiotic chromosomal processes. When integrated with additional cytological information, these results suggest a coherent model for events of the leptotene/zygotene transition, including roles for ZMM proteins and the basis for checkpoint monitoring. They also suggest that the SC plays its critical role(s) during pachytene; one possibility is discussed. We further suggest that temperature might influence chromosomal events directly, by affecting the state of the DNA, and thus the DNA/chromatin fiber.

Results

Experimental System

Cultures of wild-type and *zmm* deletion mutant diploids were taken through synchronous meiosis and examined at appropriate time points for: (1) DNA events of recombination as detected by physical assays; (2) SC formation by immunostaining of spread chromosomes with anti-Zip1 antibodies; and (3) occurrence of meiotic divisions and spore formation by standard microscopic methods. Events were examined in parallel at 33°C and 23°C. Wild-type meiosis is efficient and yields ≥95% viable spores at both temperatures (below; data not shown).

Recombination in Wild-Type Diploids at High and Low Temperature

Recombination was analyzed at the *HIS4LEU2* locus, where initiating DSBs occur at high levels at a single discrete site (Hunter and Kleckner, 2001). "Mom" and "Dad" chromosomes are marked with restriction site polymorphisms such that, following suitable restriction digestion, DNA species of interest are resolved by 1D and 2D gel electrophoresis and detected by Southern blotting with a locus-specific probe (Figures 2A–2C). At both 33°C and 23°C: (1) DSBs, SEIs, and dHJs appear and disappear in ordered succession (Figure 2D). (2) DSBs occur on ~20% of chromatids, as determined in a strain where they do not turn over (*rad50S*; Figure 2E; Alani et al., 1990). (3) Interhomolog CRs form at similar levels (18%–22%) and represent about half of all DSBs (e.g., Figure 2D). (4) Most or all remaining DSBs are resolved as NCRs, which occur at similar levels, as seen with a variant *HIS4LEU2* construct carrying markers just at the DSB site (Storlazzi et al., 1995; Figures 2B and 3C). With respect to timing, DSBs, SEIs, dHJs, and CRs all occur at earlier times at 33°C than at 23°C (Figure 2F). Most of the difference arises at the first two transitions: DSBs occur about an hour earlier and last about two-thirds as long at 33°C as at 23°C, implying both earlier onset of DSBs and more rapid exit from the DSB stage at the higher temperature (Figure 2F).

Recombination in *zmm* Mutants at High Temperature

At 33°C, all five *zmm* single mutants and four representative double mutants exhibit the same basic recombination phenotype.

A Post-DSB CR-Specific Defect

In all five single mutants, DSB formation at the assayed locus is indistinguishable from wild-type with respect to both timing and final levels, as seen in a *rad50S* background (Figure 3A). The same is true for *zip2*Δ in another background where DSB turnover is blocked (*dmc1*Δ ; Bishop et al., 1992; data not shown).

In all single and double *zmm* mutants, CRs occur at ~15% of the wild-type level (Figures 3B left, 3C, 4B, and 4C). NCRs were also analyzed, in parallel with CRs (Figure 2B). In all four examined mutants (*zip1*Δ, *zip2*Δ, *mer3*Δ, and *zip2*Δ *zip3*Δ), CRs again form at ~15% the wild-type level while NCRs form with the same levels and timing as in wild-type (Figure 3C). Thus, CR formation is specifically defective.

Thus, in *zmm* mutants at high temperature: DSBs form normally; most of the DSBs that would normally have been processed into CRs have suffered some aberrant fate; and NCRs appear to form normally, along with a small number of residual CRs.

A CR-Specific Defect at the DSB to SEI Transition

To pinpoint when the identified CR-specific defect arises in *zmm* mutants, we examined intermediate steps of recombination, i.e., DSB turnover ("exit" from the DSB stage) and appearance and disappearance of SEIs and dHJs.

In wild-type meiosis, DSBs peak at ~t = 3 hr and are essentially gone by t = 8 hr (Figure 4B, left). All *zmm* single and double mutants exhibit altered DSB patterns. Furthermore, areas under all mutant DSB curves are increased (Figure 4, legend). Assuming that DSBs form at wild-type levels in these strains (above), this feature implies an increased DSB "lifespan," which in turn implies that some or all DSBs are defective in progressing out of this stage. This DSB exit defect is manifested

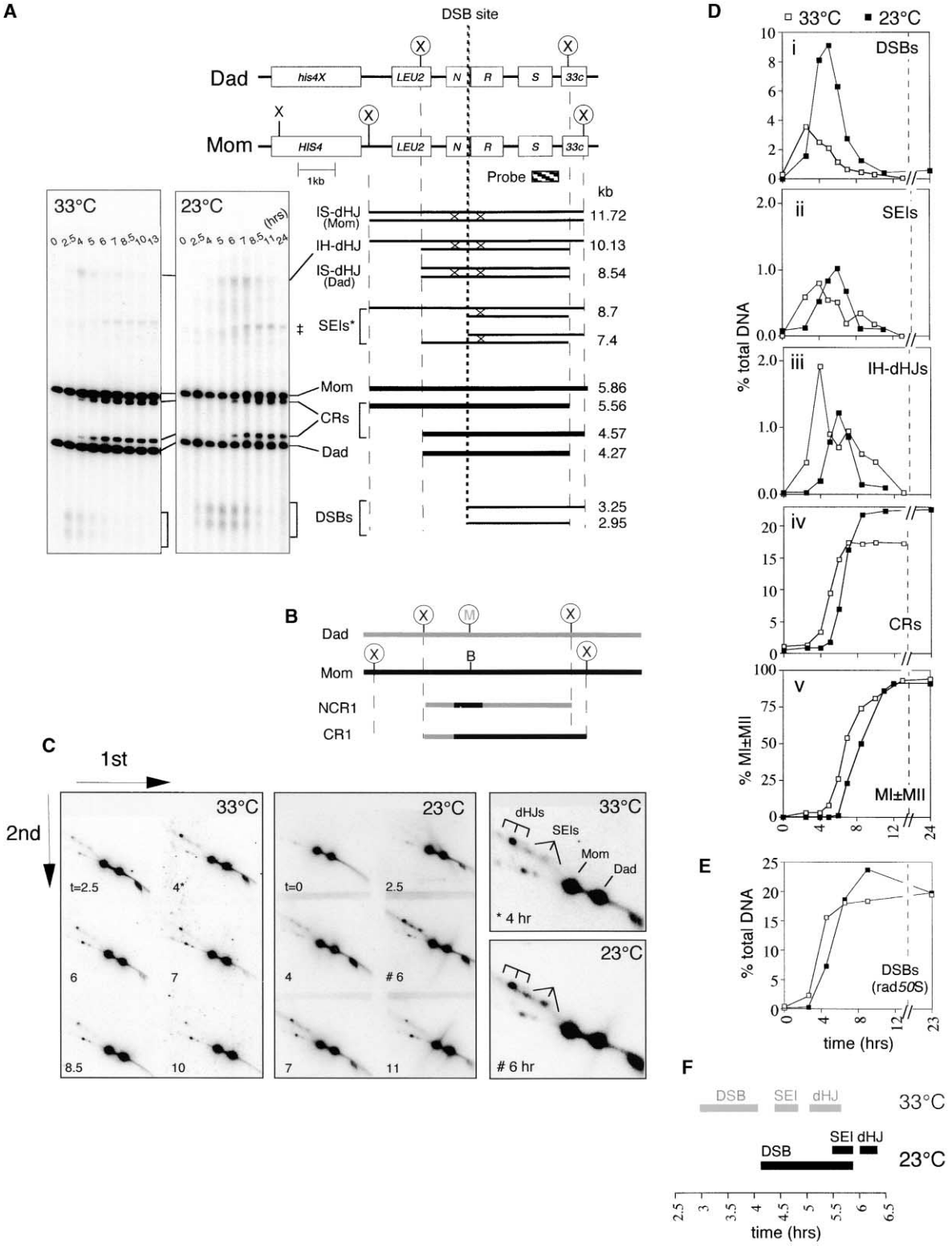

Figure 2. Wild-type Meiotic Recombination at High and Low Temperature

(A) *HIS4LEU2* locus (standard construct): open reading frames, relevant XhoI restriction sites (X), the location of the DSB site, and the probe used for Southern analysis are shown along the physical map (top; Hunter and Kleckner, 2001). Parental homologs, "Dad" and "Mom," are distinguished via restriction site polymorphisms (circled X's). Left panel: Southern blot analysis of 1D gels for representative meiotic timecourses at 33°C or 23°C. Right panel: sizes and identities of species detected in 1D or 2D gel analysis. IS-dHJs and IH-dHJs are dHJs between sisters and homologs, respectively. (*) "SEI3" and "SEI4" of Hunter and Kleckner (2001). ‡ meiosis-specific, crosshybridizing band (see Hunter and Kleckner, 2001).

(B) *HIS4LEU2*-CR/NCR tester construct. "Mom" and "Dad" homologs (black and gray lines) differ by BamHI (B) versus MluI (M) restriction

somewhat differently in different mutants. In *zip2*Δ, *zip3*Δ, and *mer3*Δ, most DSBs come and go relatively normally, but a significant fraction, about 5%–20% of total, are still present even after t = 24 hr. In *msh5*Δ, DSB levels rise to much higher than wild-type levels, suggesting that many or all DSBs are substantially delayed in progressing to later stages, and once again a significant fraction remain present at t = 24 hr. DSB levels in *zip1*Δ are moderately elevated at late times, implying a modest defect in progression, but all DSBs do eventually disappear. DSB patterns of each double mutant are hybrids of the two component single mutant patterns (Figure 4C).

SEI formation is altered dramatically in all *zmm* mutants (Figures 4B and 4C). In *zip3*Δ, *mer3*Δ, *msh5*Δ, and all four analyzed double mutants (*zip2*Δ*zip1*Δ, *zip3*Δ*zip1*Δ, *zip2*Δ*zip3*Δ, and *msh5*Δ*zip1*Δ), maximum steady state levels of SEIs are at or below the level of detection, ≤15% of wild-type. In *zip2*Δ, SEIs reach ~30% the wild-type maximal level. In *zip1*Δ, SEIs eventually reach wild-type maximum steady state levels, but form with a severe delay, also seen for residual SEIs in other mutants. All *zmm* mutants also exhibit aberrant dHJ patterns, with the dHJ curve for each mutant directly mirroring the corresponding SEI curve (Figure 4B), and with appearance of dHJs delayed relative to the time of appearance of SEIs by ~2 hr.

These results imply that all *zmm* mutants are specifically defective in converting DSBs to SEIs, as seen in (1) longer DSB lifespan, (2) residual DSBs present at late times, (3) delayed appearance of SEIs, and/or (4) severely decreased SEI levels. dHJ patterns then mirror SEI patterns. Since NCR formation is apparently normal under these conditions (above), this DSB-to-SEI defect appears to pertain specifically to the formation of CRs. This suggests that DSBs have been differentiated into two types: those destined to yield CRs and those destined to yield NCRs, and there appears to be a specific defect in progression of the CR-designated DSBs to SEIs.

CR-Designated DSBs Disappear

A striking further feature of the above patterns is that the subset of DSBs that would normally have yielded the missing CRs have largely disappeared from the assay system. By t = 24 hr, 10%–40% can be accounted for as persisting DSBs (Figure 4); however, the majority are not present as "stuck" DSBs, SEIs, or dHJs (Figures 4B and 4C), additional NCRs (Figure 3), or discrete aberrant species in 1D or 2D gels (data not shown). The corresponding DNA molecules may be degraded, present in undetected intermediates, and/or processed into undetected atypical products, e.g., by undetected interaction with a sister chromatid. This feature suggests that CR-designated DSBs are specifically blocked from proceeding toward any regular interhomolog fate and are then processed in various aberrant ways. In most cases, SEIs and dHJs are virtually absent. In *zip1*Δ, SEIs and dHJs do reach significant steady state levels. However, these SEIs/dHJs are still not contributing any additional CRs, which occur at the same low level in *zip1*Δ as in other mutants. There may be only a very few SEI and dHJ molecules in *zip1*Δ, as in other cases, but these few may persist for a very long period of time, and thus accumulate to significant steady state levels while not contributing significantly to CRs. Alternatively, a higher number of SEIs/dHJs may occur, but then be resolved into undetected interhomolog products, e.g., unassayed types of NCRs. Regardless of which explanation is correct, in *zip1*Δ, as in all other *zmm* mutants, the primary defect is progression of CR-designated DSBs beyond the DSB stage to SEIs, thus resulting in quantitatively and/or qualitatively altered SEI/dHJ formation.

Recombination in *zmm* Mutants at Low Temperature

At 23°C, all *zmm* mutants again exhibit the same basic recombination phenotype, which is, however, qualitatively different from that observed at 33°C.

Interhomolog Products Form at High Levels but with Decreased CRs and Increased NCRs

All five *zmm* single mutants exhibit normal levels of DSBs in a *rad50S* background (Figure 3A). There is also a tendency for DSBs to appear at higher than wild-type levels at earlier than normal times (Figure 3A; G.V.B., unpublished data).

In all five single mutants and all analyzed double mutants, (*zip1*Δ, *zip2*Δ, *zip3*Δ, *mer3*Δ, *msh5*Δ, *zip2*Δ*zip1*Δ, *msh5*Δ*zip1*Δ, *zip3*Δ*zip1*Δ), CRs form at ~40%–50% of the wild-type level and appear with a delay of ~5 hr (Figures 3B, right, and 5). NCRs initially appear at relatively normal levels at normal times; however, rather than reaching a plateau at ~10 hr as in wild-type, they continue to appear, ultimately reaching several times the wild-type level (Figure 3C, ii). Thus, both CRs and NCRs occur at substantially higher levels at low temperature than at high temperature (above) but with a subset

polymorphism at a central position (see [A]). Southern blot analysis after restriction digest with XhoI plus MluI detects six product bands. Among these, CR1 and NCR1 derive almost exclusively from, and thus are taken to represent, CRs and NCRs, respectively (Storlazzi et al., 1995).

(C) Southern analysis of 2D gels showing representative time points from the timecourses shown in (A). Panels on the right show enlarged details of time points shown at left.

(D) Quantitative analysis of the two wild-type timecourses at 33°C and 23°C shown in (A) and (C). DNA species (in i–iv) are given as percent of total hybridizing signal in the corresponding lane, as a function of time after transfer to sporulation medium at t = 0. %MI±II, percentage of cells that have completed one or both nuclear divisions as determined by DAPI staining (Experimental Procedures). Time axes interrupted at 13 hr ("//").

(E) DSB formation in a *rad50S* background at 33°C and 23°C.

(F) Timing of DNA events from timecourses shown in (A), (C), and (D). Start and end points of each bar designate the time when 50% of the initiated recombination events have entered or exited the corresponding stage, calculated by cumulative analysis of primary data (Hunter and Kleckner, 2001). Calculations assume that: (1) maximal *rad50S* DSB levels represent the total number of initiated events and (2) SEIs and dHJs are CR-specific intermediates (below). Average lifespans determined in four timecourses at 33°C and 23°C, respectively, are 60 ± 7 min (±1 SD), and 95 ± 14 min (±1 SD) (O. Nanassy and N.K., unpublished data).

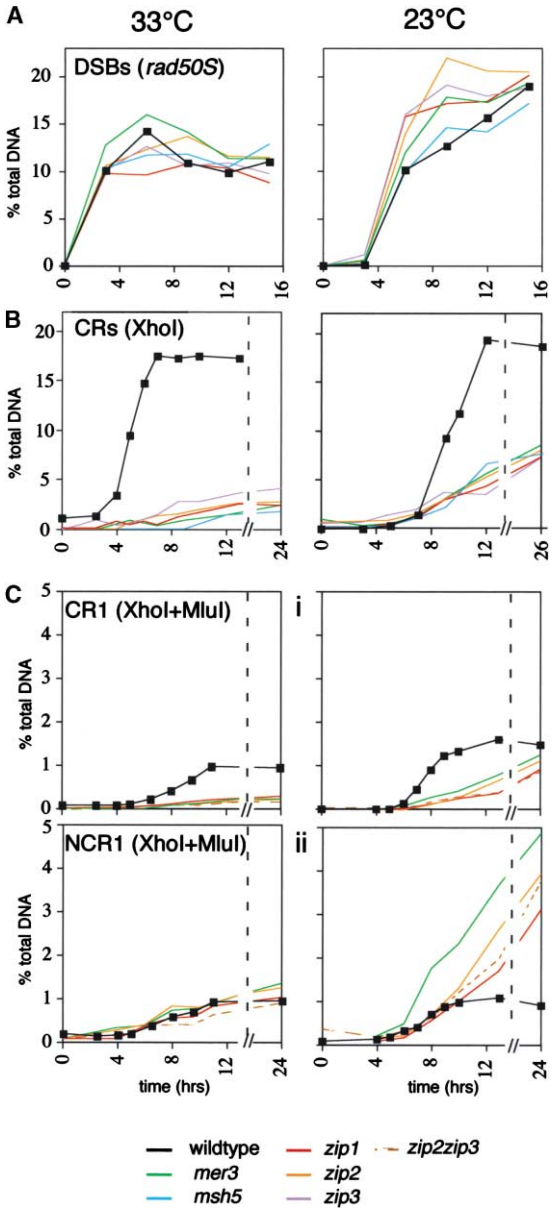

Figure 3. DSBs, CRs and NCRs in *zmm* Mutants at High and Low Temperature

Wild-type and *zmm* mutant strains were examined at 33°C and 23°C for recombination as described in Figure 2.

(A) DSB formation assayed with the *HIS4LEU2* standard construct in a *rad50S* strain background.

(B) CR formation assayed with the standard *HIS4LEU2* construct.

(C) CRs (i) and NCRs (ii) assayed with the CR/NCR tester construct. Maximal levels of CR1 and NCR1 are 0.9% and 0.9% (at 33°C) and 1.6% and 1.1% (23°C).

of products appearing much later than normal. This difference suggests that, at low temperature, in contrast to high temperature, most or all DSBs are progressing to regular interhomolog products, but with some delay(s) and with aberrant partitioning between the two types such that CRs are reduced and NCRs are increased.

A Defect at the DSB to SEI Transition

In *RAD50* timecourses, DSBs in *zmm* mutants appear at normal times, peak at steady state DSB levels similar to wild-type, and turn over efficiently. No significant fraction of DSBs remain "stuck" at very late times in any mutant, beyond a low level also seen in wild-type (Figures 5A and 5B), but areas under DSB curves are larger than for wild-type, particularly in the double mutants (*zip2*Δ*zip1*Δ, *msh5*Δ*zip1*Δ, *zip3*Δ*zip1*Δ; Figure 5D), where the increase is 60%–80%, and in all single mutants except *mer3*Δ. Thus, in most cases, some or all DSBs are modestly but significantly delayed in exiting that stage. In several single mutants, an exaggerated shoulder of DSBs is present at later times (Figure 5B), suggesting delayed turnover of only a subset of DSBs, perhaps in correlation with delayed appearance of a subset of products (Discussion).

SEIs appear at substantial steady state levels in all *zmm* mutants and then disappear. However, all mutants exhibit aberrant SEI patterns, of two alternative types. In a *mer3*Δ single mutant and two double mutants that do not contain the *mer3*Δ mutation, *msh5*Δ*zip1*Δ and *zip2*Δ*zip1*Δ, SEIs form with roughly wild-type timing but at about half the wild-type steady state level (Figures 5B and 5C). In *zip1*Δ, *zip2*Δ, *zip3*Δ, and *msh5*Δ single mutants, SEIs are present at maximal steady state levels similar to wild-type but are present at such levels at much later than normal times (Figures 5B and 5C). dHJ patterns are also defective in all *zmm* mutants, with the dHJ curve of each mutant mirroring its corresponding SEI curve (Figures 5B and 5C).

Synthesis

zmm mutants exhibit an aberrant DSB to SEI progression and an aberrant array of CRs and NCRs at both 33°C and 23°C, but with significant differences between the two cases. At 33°C, differentiation of DSBs into CR and NCR types is robust but there is a specific block in the progression of CR-designated DSBs toward their assigned fate, with the affected DSBs either remaining as such or progressing to unknown intermediates or products (above). In contrast, at 23°C, progression beyond the DSB stage is delayed, but all DSBs do eventually disappear. Furthermore, most or all DSBs subsequently appear in regular interhomolog products, with effects on both CRs (which are decreased) and NCRs (which are increased), but with hints of two subpopulations of both DSBs and products.

Onset of SC Formation Is Defective in *zmm* Mutants at Both High and Low Temperature

Zip1 installation onto meiotic chromosomes was examined in wild-type and non-*zip1*Δ *zmm* mutants in parallel, at 23°C and at 33°C. At appropriate time points, chromosomes were spread and stained with anti-Zip1 antibodies. All observed staining is Zip1 specific (data not shown).

Wild-Type Meiosis

Wild-type nuclei with significant Zip1 staining fall into three major classes (Figure 6A). Class I nuclei (green) exhibit only foci of Zip1 staining, 3 to 20 per nucleus, over the chromatin. Class II nuclei (medium blue) exhibit substantial Zip1 staining present in continuous lines or rows of foci on a subset of chromosomes. Class III nuclei (red) exhibit what appears to be a full genome complement of staining, either as smooth continuous lines or as rows of bright patches connected by regions of lesser

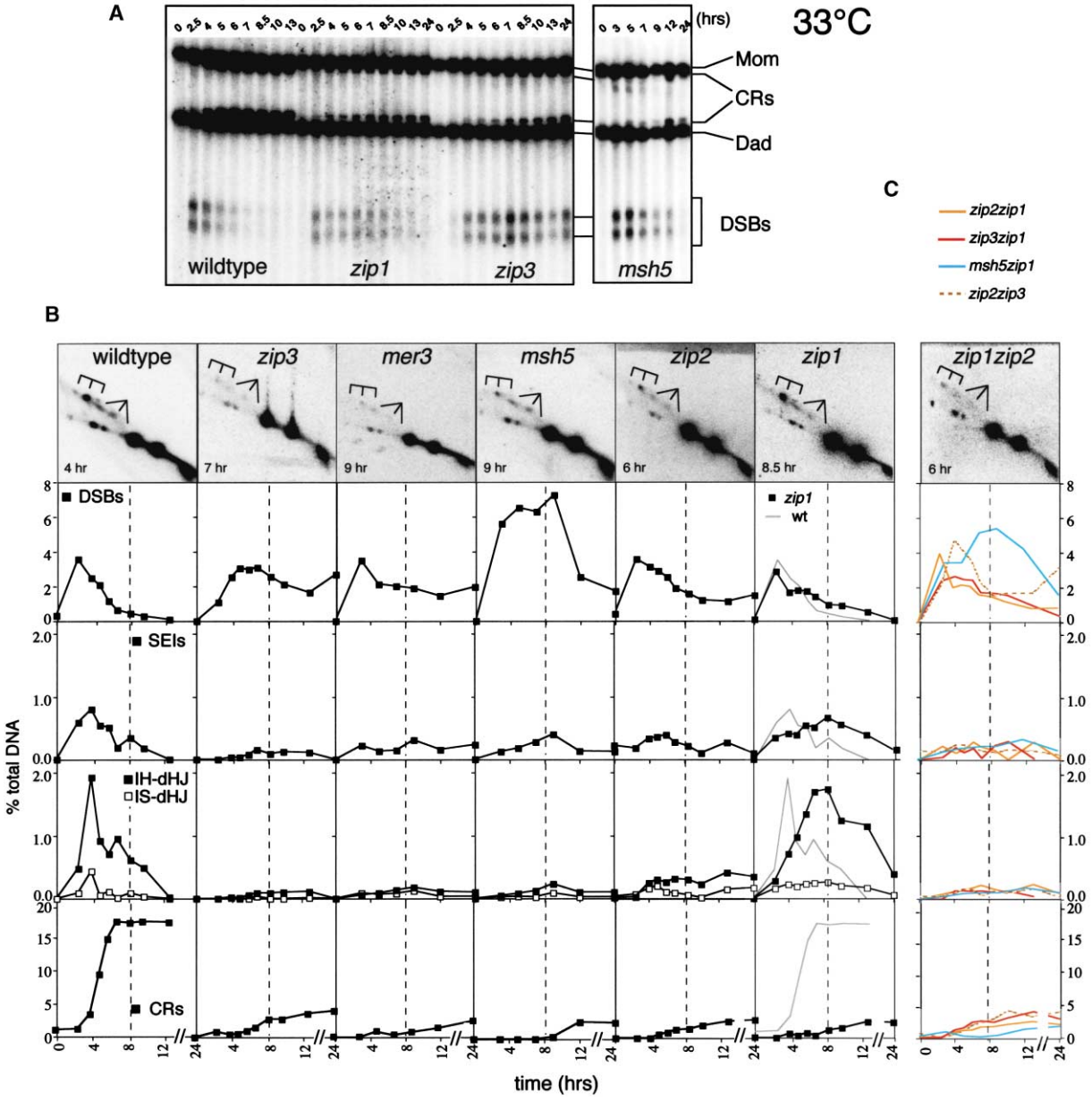

Figure 4. Recombination Intermediates in *zmm* Mutants at High Temperature (33°C)

(A) One-dimensional gels showing representative timecourses of wild-type, *zip1*Δ, *zip3*Δ, and *msh5*Δ. The same timecourses are quantitated in (B).

(B and C) Quantitative analysis of DNA events in wild-type and indicated *zmm* single mutants (B) and double mutants (C) in representative timecourses. Top row: 2D gels for time points exhibiting maximal SEI/dHJ levels. Below: levels of indicated DNA species as percent of total hybridizing signal over time after transfer to sporulation medium. For comparison, gray lines in the *zip1*Δ panels show corresponding wild-type data. Dashed vertical line marks the 8 hr time point. Average minimum lifespans of DSBs are 0.9 hr (wild-type), 2.7 hr (*zip3*Δ), 1.5 hr (*mer3*Δ), 4.7 hr (*msh5*Δ), 2.1 hr (*zip2*Δ), 1.1 hr (*zip1*Δ), 1.7 hr (*zip2*Δ*zip1*Δ), 2.7 hr (*zip3*Δ*zip1*Δ), 4.3 hr (*msh5*Δ*zip1*Δ), and 3.0 hr (*zip2*Δ*zip3*Δ); persistence beyond final time point not considered.

staining. Class I, class II, and class III nuclei appear in succession during prophase at both 23°C and 33°C (Figure 6B, top). Class I nuclei represent preleptotene/leptotene: they occur very early and are also seen in mutants lacking DSBs (Henderson and Keeney, 2004). Class II and class III nuclei correspond to zygotene (partial SC) and pachytene (full SC), respectively. At 33°C (but not 23°C), class II nuclei are also present after pachytene (Figure 6B), perhaps as intermediates in SC disassembly under this condition.

zmm *Mutants*

All four non-*zip1 zmm* single mutants are distinctly defective for SC formation at both 33°C and 23°C (Figures 6A, 6C, and 6D). (1) Pre-leptotene/leptotene nuclei (class I) appear and disappear similarly as in wild-type. However, there is a tendency for class I nuclei to appear at

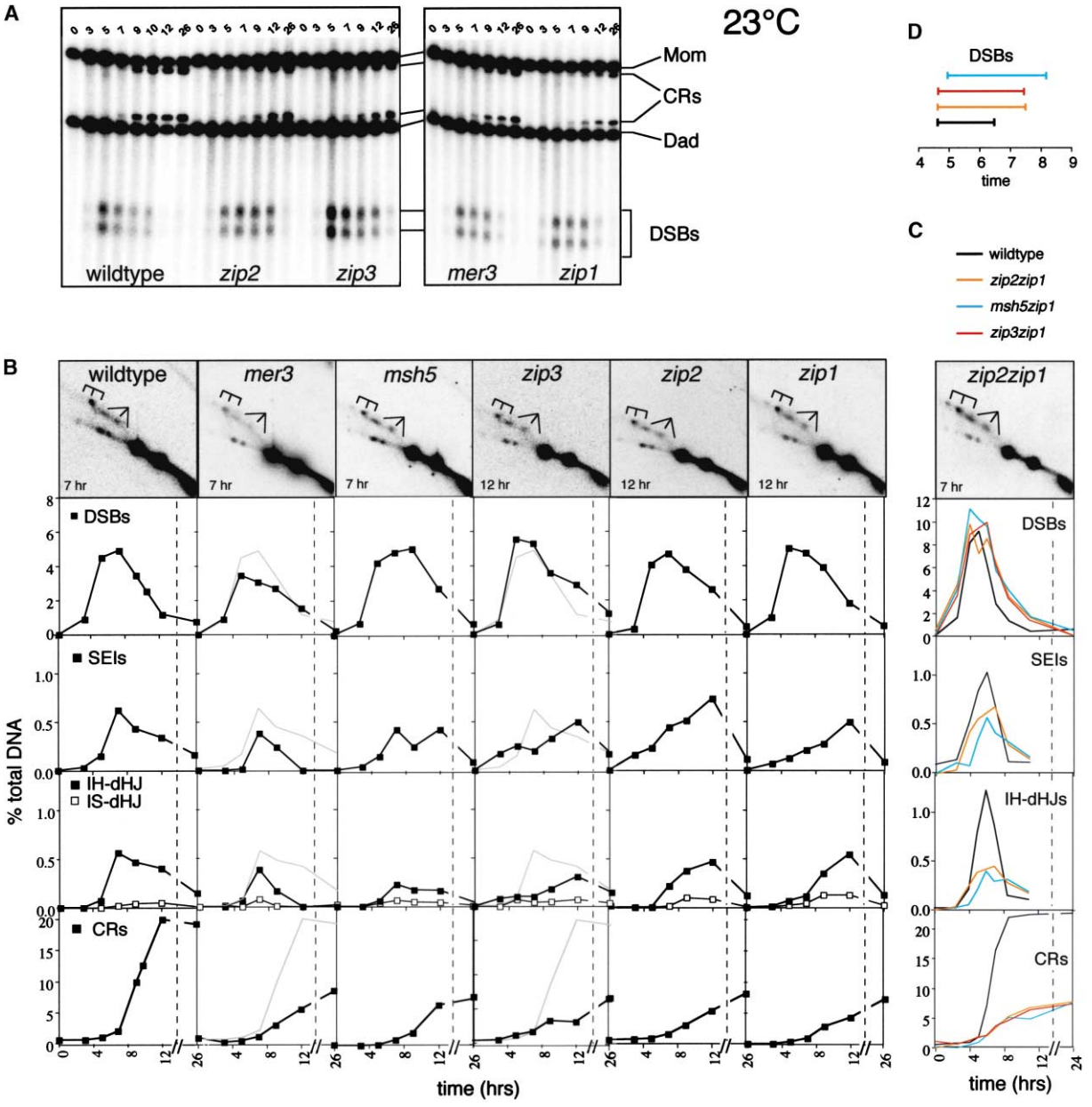

Figure 5. Recombination Intermediates and Products in *zmm* Mutants at Low Temperature (23°C)

(A) One-dimensional gels showing representative timecourses of wild-type, *zip2*Δ, *zip3*Δ, *mer3*Δ, and *zip1*Δ. Quantitative analysis of the same timecourses is shown in (B).

(B and C) Quantitative analysis of DNA events in *zmm* single and double mutants, analogous to Figures 3B and 3C. Dashed line = interruption of the timeline. Average minimum DSB lifespans are 1.9 hr (wild-type), 2.7 hr (*zip3*Δ), 1.5 hr (*mer3*Δ), 2.4 hr (*msh5*Δ), 2.2 hr (*zip2*Δ), 2.1 hr (*zip1*Δ) (B); 1.8 hr (wild-type), 3.2 hr (*msh5*Δ*zip1*Δ), 2.9 hr (*zip2*Δ*zip1*Δ), 2.8 hr (*zip3*Δ*zip1*Δ). Slower kinetics in (A) and (B) relative to (C) and Figure 2 reflect early use of a suboptimal pre-sporulation regimen; all mutants show the same patterns with the optimal standard protocol (data not shown).

(D) DSB lifespans calculated for the timecourses from Figure 5C (as in Figure 2F).

higher than normal levels at later than normal times, particularly at 23°C (Figure 6D, green), implying delayed onset of SC formation. (2) Some normal-looking zygotene nuclei then appear (class II; Figure 6D, medium blue). Concomitantly, however, nuclei accumulate in aberrant morphological classes I and II (Figure 6A, wavy; dark gray; light blue; light gray; dark red; Figure 6D, lower three lines). Morphologically normal pachytene nuclei are either absent or are rare and appear only at very late times (Figure 6D, red). These patterns suggest that SC formation is defective from its earliest stages onward, but with partial or aberrant Zip1/SC installation still occurring in many nuclei. Normal SC also fails to occur with normal timing in *zip2*Δ, *zip3*Δ, and *msh4*Δ as assayed at 30°C in diverse strain backgrounds and sporulation conditions (Chua and Roeder, 1998; Novak

et al., 2001; Agarwal and Roeder, 2000). (3) Many mutant nuclei contain a brightly staining aggregate of Zip1 protein, a polycomplex (PC) (e.g., Figure 6A). PCs are rare in wild-type yeast meiosis (e.g., Figure 6C) but accumulate characteristically when SC morphogenesis is aberrant (reviewed by Zickler and Kleckner, 1999). Nuclei containing PCs begin to appear in *zmm* nuclei at the time of the leptotene/zygotene transition, again implying that SC formation is defective from its earliest stages. PCs increase in abundance thereafter until, finally, a PC is present in the majority of nuclei, with or without chromosomal staining (Figure 6C). (4) Interestingly, underlying chromosome morphology is also often abnormal in *zmm* nuclei, as indicated by Zip1 staining in multiple foci not connected by lines (Figure 6A, "dark gray"), very stringy staining (Figure 6A; "wavy"), or highly contracted, wiggly Zip1 lines (Figure 6A, most "light blue" and "dark red").

The findings of delayed leptotene exit, concomitant appearance of aberrant and apparently normal zygotene morphologies, and early appearance of PCs all point to a specific defect in the timely onset of SC formation, rather than simply a defect in installation of the structure per se (Discussion).

In *zmm* Mutants, Recombination and Progression Phenotypes Vary Coordinately in Different Conditions

In wild-type cells, the two meiotic divisions occur efficiently and similarly at both 23°C and 33°C (Figure 2D, v; Figure 7A). In contrast, each of the five single *zmm* mutants and several representative double mutants (*zip2*Δ*zip1*Δ, *zip3*Δ*zip1*Δ, *msh5*Δ*zip1*Δ, *zip2*Δ*zip3*Δ) show the same progression defect; and this defect is qualitatively different at the two temperatures. At 33°C, >85% of cells arrest before occurrence of division I (e.g., Figure 7A, left) and do not form spores (Figure 7B, 33°C). At 23°C, >90% of cells complete division I but only after a substantial delay of 3 to 7 hr (e.g., Figure 7A, left); most cells also continue through meiosis II and make spores (Figure 7B, left; data not shown). Thus, meiotic progression phenotype (arrest at high temperature and delayed but efficient progression at low temperature) mirrors meiotic recombination phenotype (a severe CR-specific block at high temperature and slow but efficient progression to CRs and NCRs at low temperature) (see also Nakagawa and Ogawa, 1999). We refer to these two recombination/progression phenotypes as "Mode H" and "Mode L," respectively.

In a previous study, under the same conditions used here but at the intermediate temperature of 30°C, a *zip1*Δ mutant exhibits what we can now see to be a mixture of Mode H and Mode L phenotypes with respect to both recombination and cell cycle progression (Storlazzi et al., 1996): intermediate levels of both CRs and NCRs are formed and half of cells undergo permanent cell cycle arrest (as at 33°C) while the other half progresses with a several hour delay (as at 23°C).

These results suggest that the two recombination modes described here for 23°C and 33°C represent two discrete alternatives such that, at an intermediate temperature, a mixture of the two situations is observed, rather than a continuous transition. We infer that recombination mode determines the progression phenotype (Discussion). Since a given cell exhibits either arrest or delay, progression mode is also selected as a binary choice between two discrete alternatives. Thus, for example, per-cell choices of recombination mode, occurring differently at different loci throughout the genome, might be integrated by surveillance components, which would then trigger either one response or the other. Studies at intermediate temperature further reveal that recombination/progression mode can be modulated by sporulation conditions: SK1 *zip1*Δ at 30°C in this same strain background exhibits a mixed phenotype in the low KAc sporulation medium used here, but a pure Mode L phenotype in high KAc sporulation medium (Sym et al., 1993; Sym and Roeder, 1994; Storlazzi et al., 1996; G.V.B., unpublished data), suggesting that at intermediate temperature, sporulation conditions can tip the balance between the two modes.

We also investigated Mode L/Mode H temperature thresholds for all *zmm* mutants, over a wide range of temperatures, by analyzing spore formation, which is absent due to progression arrest in Mode H and present in Mode L and which can be conveniently assayed via spore wall fluorescence in patches of sporulated cells (Figure 7B). Interestingly, different *zmm* mutants exhibit the transition from spore formation to no spore formation at different threshold temperatures (left panel). This result implies that, at intermediate temperature, residual ZMM proteins are having significant effects, which are somewhat different in different single mutants. Also: (1) A *msh4*Δ mutant exhibits the same temperature threshold as a *msh5*Δ mutant, as expected from Msh4/Msh5 collaboration (Introduction) and (2) *dmc1*Δ, defective in a meiotic RecA homolog, exhibits a phenotype similar to Mode H: a severe block to DSB turnover plus prophase arrest and/or ≤ 5% spore formation at all temperatures (Bishop et al., 1992; Figure 7B; G.V.B., unpublished data).

All experiments described above involve the SK1 strain background. *zmm* mutants were initially characterized and/or have been studied extensively in the "BR" background (Sym et al., 1993; Chua and Roeder, 1998; Agarwal and Roeder, 2000). In BR, as in SK1, recombination and progression/spore formation phenotypes remain linked. (1) BR *zip1*Δ arrests at all temperatures (Figure 7B) and exhibits a severe reduction of CRs by physical assay at 30°C (Sym et al., 1993) and at 34°C (G.V.B., unpublished data), i.e., a Mode H phenotype. (2) BR *zip3*Δ forms spores at low temperature but not at high temperature (Figure 7B) and, at intermediate temperature, exhibits a "mixed" phenotype for both (genetic) recombination and progression (Agarwal and Roeder, 2000). (3) BR *dmc1*Δ arrests at high temperature but, at lower temperatures, exhibits progression delay and, by genetic criteria, Mode L-like recombination (Figure 7B; Rockmill et al., 1995). Furthermore, comparison of *zip3*Δ, *zip1*Δ, and *dmc1*Δ phenotypes in the BR and SK1 strain backgrounds reveals that all three mutants exhibit different absolute and relative temperature thresholds in the two cases (Figure 7B, colored bullets). Thus, the probability that a particular mutant will exhibit a Mode H or Mode L phenotype is also influenced by strain background.

Yeast *zmm* mutants have previously been examined only at 30°C in diverse strain backgrounds and sporulation conditions. In genetic studies, all mutants exhibited

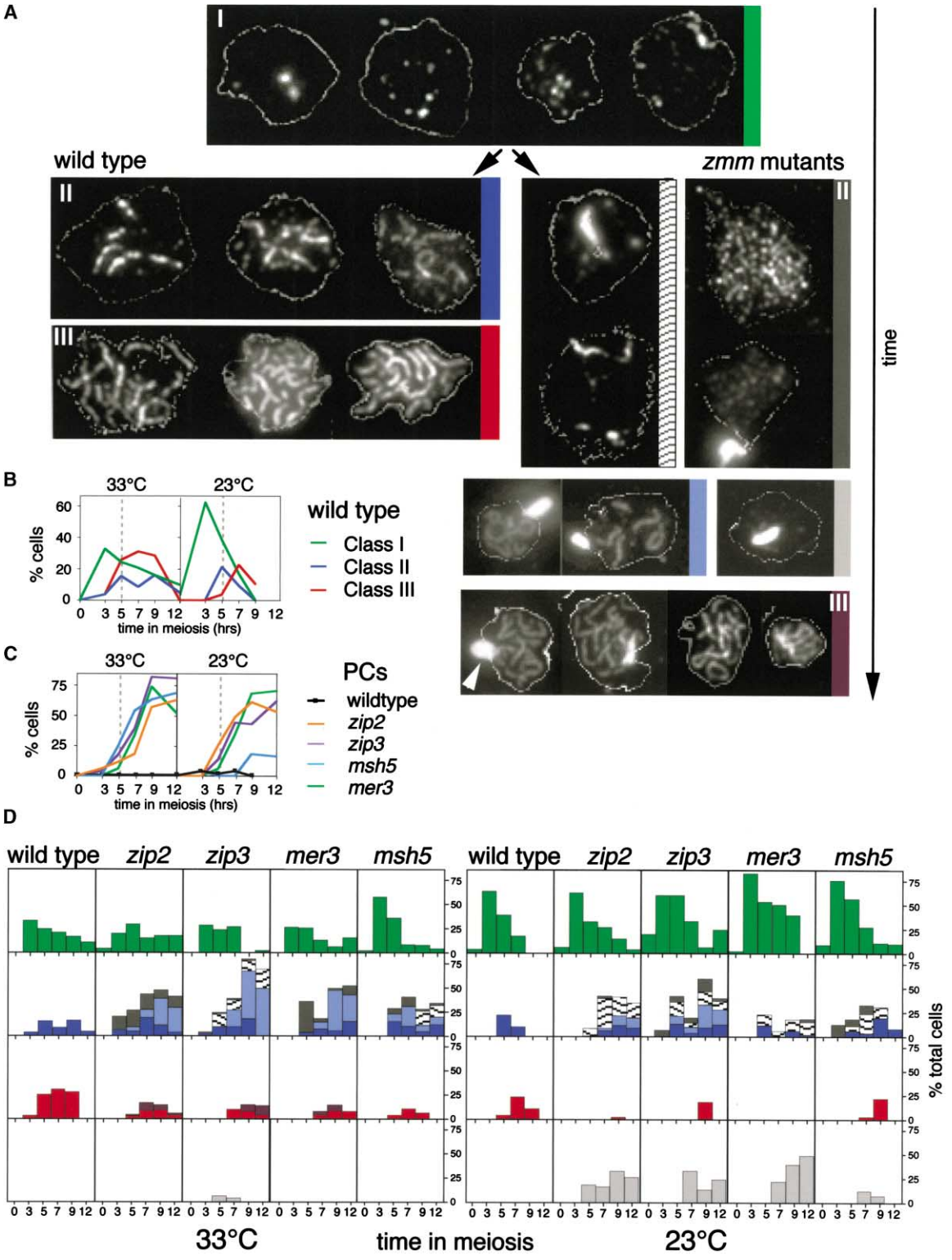

Figure 6. Zip1 Loading in *zmm* Mutants

(A) Representative images of surface spread nuclei immunostained with anti-Zip1 antibody. Top and left, wild-type morphologies. Class I: S phase/leptotene (3 to 20 foci); class II: zygotene (few to several lines or dots-in-lines of Zip1 staining); class III: pachytene (continuous lines or dots-in-lines of Zip1 staining on most or all chromosomes). Right: aberrant morphologies frequently observed in *zmm* mutants. Class II*: Zip1 localization to parts of the genome and/or a PC. One to three string-like objects (wavy lines); multiple (>20) foci without clear underlying structure (dark gray); class II-like but containing a polycomplex (light blue); polycomplex only without significant chromosomal staining (light gray). Class III*: apparent staining of the entire chromosome complement; multiple lines, often very flexible looking, with or without polycomplex (white arrowhead).

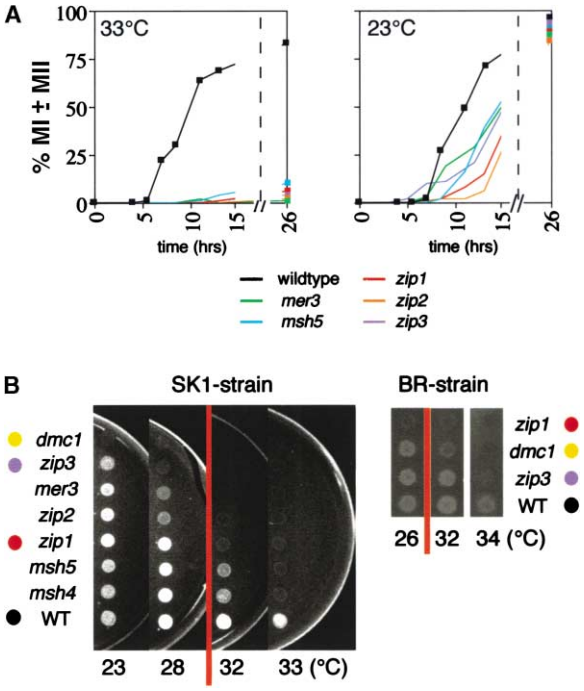

Figure 7. Meiotic Cell Cycle Progression in *zmm* Mutants

(A) %MI±MII = percentage of cells that have completed one or both meiotic divisions as determined by DAPI staining. Dashed line = interruption of time line.

(B) UV fluorescence of cell patches arising after incubation on solid sporulation medium for 4 days in SK1 or BR strains. Orange line indicates 30°C, the standard temperature for yeast studies. Colored bullets mark *zmm* mutations analyzed in both strain backgrounds.

high levels of recombination between markers within a single gene, thus implying high total levels of recombination initiation (i.e., DSBs) and a robust preference for interhomolog recombination over intersister recombination. Genetic and physical studies also revealed reductions in CRs, but with striking differences in residual levels and with differences in meiotic progression phenotypes. Each previously reported 30°C mutant phenotype can now be explained by the appropriate combination of the two discrete recombination/progression modes described at 23°C and 33°C above: severely decreased CRs, normal NCRs, and cell cycle arrest (Mode H) or modestly decreased CRs, elevated NCRs, and delayed but efficient cell cycle progression (Mode L). For example, at 30°C, the *zip1*Δ phenotype is Mode H in BR/high KAc, Mode L phenotype in SK1/high KAc, and a mixture of Mode H and Mode L in SK1/low KAc medium. These complexities may explain why such diverse phenotypes have previously been observed in *zmm* mutants.

Discussion

Phenotypes of *zmm* mutants reveal several new features of meiotic recombination, the relationship between recombination and SC formation, role(s) of ZMM proteins, and the nature of meiotic prophase checkpoint surveillance. These findings lead to new models for crossover control and the role of the SC. A positive role for higher temperature in promoting early meiotic recombination-related events is also revealed.

CR/NCR Differentiation Precedes Onset of Stable Strand Exchange

At high temperature, *zmm* mutants exhibit normal levels of DSBs and NCRs but strong coordinate defects in SEIs, dHJs, and CRs. Thus, the CR/NCR decision is made very early in the recombination process, prior to SEI formation, and therefore prior to onset of stable strand exchange. Decision making is likely imposed upon already formed DSBs, with onset of stable strand exchange as an immediate downstream outcome (Figure 8A; below). This timing has two important implications: first, regulation is imposed between two major biochemical steps such that decision making can be immediately implemented and locked in by ensuing chemical changes. Second, the onset of stable strand exchange is the critically regulated step.

The high temperature *zmm* phenotype further implies that SEIs, as well as dHJs (Allers and Lichten, 2001), are CR-specific intermediates. Since SEIs and dHJs are the only discrete post-DSB recombination intermediates identified to date, the molecular events leading from DSBs to NCRs remain to be defined (Figure 8A). Current evidence is consistent with the idea that NCRs arise by a synthesis-dependent strand-annealing mechanism (SDSA; Allers and Lichten, 2001). We favor the idea that SDSA proceeds via strand exchange intermediates that are evanescent and/or comprise only very short stretches of heteroduplex, thus rendering them undetectable by our methods. However, the possibility that NCRs arise via very evanescent SEIs and dHJs cannot be excluded.

Ultimately, *zmm* mutants at high temperature form ~15% of the wild-type level of CRs; these events are independent not only of ZMM proteins but also of SEIs and dHJs. We suggest that this class of CRs also occurs during wild-type yeast meiosis and may well be equivalent to the Msh5-independent crossovers recently defined by de los Santos et al. (2003). Linkage analysis in yeast identifies ~90 CRs per meiotic nucleus while cytological correlates, i.e., late nodules and ZMM immunostaining foci, both average ≤70 per nucleus (Byers and Goetsch, 1975; Rockmill et al., 2003). Approximately fifteen percent of ZMM-independent CRs would explain this discrepancy. Formation of NCRs is also independent of ZMMs, SEIs, and dHJs. Thus, these extra CRs could arise as a minority product along the NCR or "default" branch of the meiotic recombination pathway (Figure 8A). Interhomolog recombination in mitotic yeast cells similarly yields mostly NCRs plus ~10% CRs (Paques and Haber, 1999). On the other hand, in mouse, mitotic interhomolog recombination yields only NCRs

(B) Percentages of nuclei in each Zip1-staining category over time in wild-type strains at 23°C and 33°C.

(C) Percentages of nuclei containing a PC over time in wild-type and *zmm* mutants at 23°C and 33°C.

(D) Percentages of nuclei in different morphological categories over time in wild-type and *zmm* mutants at 33°C and 23°C. For every time point, 50 or more nuclei were photographed and scored. Categories defined and color-coded as in (A).

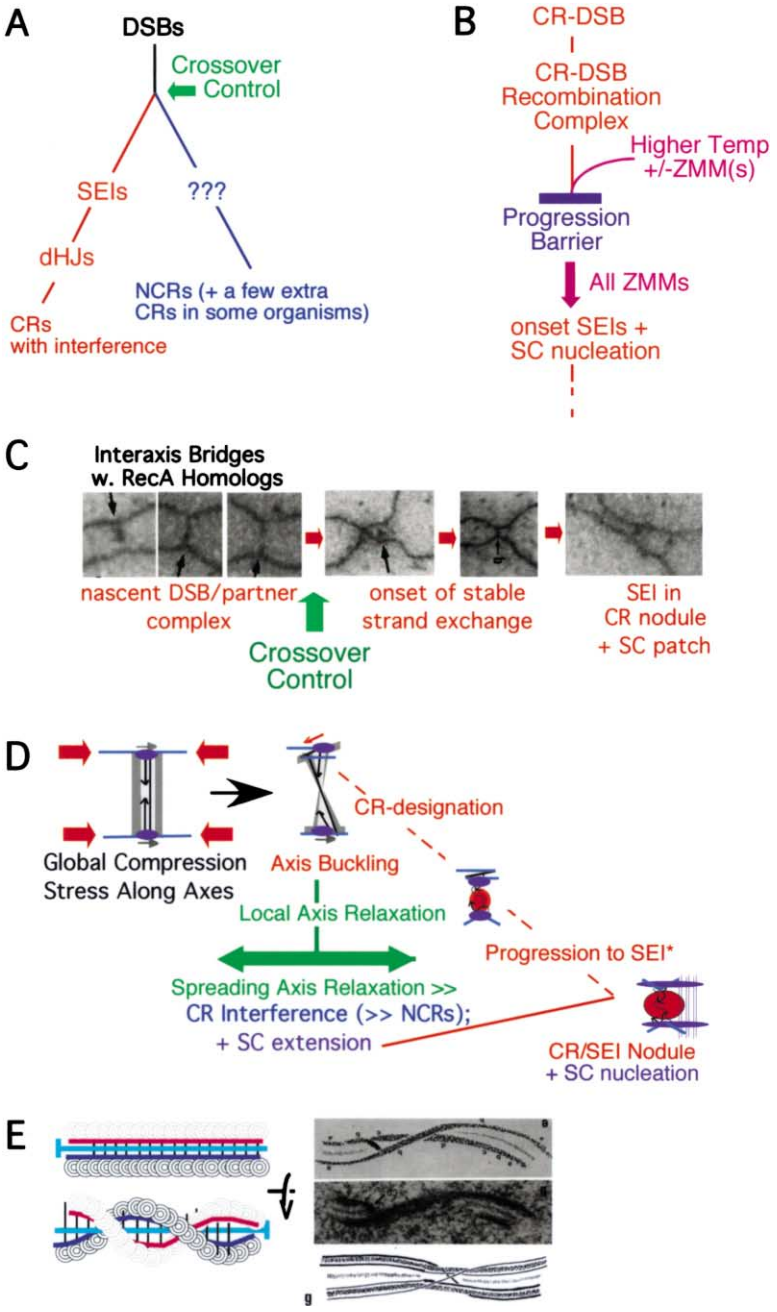

Figure 8. Models for Meiotic Recombination, Crossover Control, SC Formation, and the Role of the SC

(A) A single bifurcating pathway of meiotic recombination.

(B) CR designation leads to SEI formation and nucleation of SC in wild-type meiosis via steps defined by *zmm* mutant phenotypes. Final outcome is a coupled coordinate transition that takes CR-DSBs to SEIs and results in nucleation of SC, dependent upon all ZMMs working together in mechanistic linkage. At 33°C in *zmm* mutants, all steps through progression barrier occur normally; in the absence of one or more ZMMs, progression beyond that point is blocked resulting in coordinate defects at the DNA and SC levels. At 23°C in *zmm* mutants, progression barrier is abrogated. CR-DSB recombination complex progresses outside of the normal coupled process resulting in efficient but aberrant progression of CR-DSBs (see text) and absence of SC nucleation. By implication, the progression barrier can be promoted by higher temperature alone (in the absence of ZMMs) but, at lower temperature, requires all ZMMs. At intermediate temperatures, the threshold for the switch from Mode L to Mode H represents the probability that the progression barrier will form correctly. Since single *zmm* mutants exhibit different temperature thresholds, residual ZMMs present in those mutants have different residual capacities to collaborate with "residual temperature" to promote this step.

(C) Composite model for events of leptotene/zygotene. Images of *Allium* chromosomes (Albini and Jones, 1987 and G.H. Jones, personal communication). At late leptotene, presynaptically coaligned homolog axes are linked at a distance of ~400 nm by interaxis bridges decorated by RecA homologs (e.g., Tarsounas et al., 1999). Bridges then disappear. At some such sites, preferentially those designated to mature into CRs (Introduction), patches of SC containing CR-correlated nodules appear. DNA events are indicated by analogy with yeast (Figure 1E; text).

(D) Mechanical model for crossover control at the bridge stage and ensuing SC formation (see text).

(E) Left: diagrammatic representation of SC twisting. Right: twisted segment of rat pachytene SC showing reciprocal exchange of chromatid axes (Moens, 1978).

(Johnson and Jasin, 2000). Thus, the NCR branch of the meiotic recombination pathway could be derived from mitotic interhomolog recombination, whose nature then determines whether the meiotic process does exhibit "extra" CRs (as in yeast and perhaps *Arabidopsis*) or not (as in *C. elegans* and perhaps in mouse) (Edelmann et al., 1999; Kelly et al., 2000; Copenhaver et al., 2002).

Interference Does Not Require SC Formation but SC Formation May Require Interference

In wild-type meiosis, the distribution of DSBs between CRs and NCRs presumably reflects the combined effects of CR designation and interference (further discussion below). At high temperature, *zmm* mutants form normal levels of NCRs. Thus, by implication, crossover control decision making, including interference, has occurred in *zmm* mutants at high temperature. *zip1*Δ is devoid of SC, and all other *zmm* mutants exhibit delayed onset of and/or defects in SC formation. Taken together, these considerations suggest that crossover control, including interference, is entirely independent of the SC.

Current cytological data now lead to the same conclusion. In wild-type meiosis, immunostaining foci of ZMM proteins appear at zygotene/early pachytene, are correlated with crossovers, and show an "interference distribution" along pachytene chromosomes, suggesting that they mark the sites of future CRs (Henderson and Keeney, 2004; Fung et al., 2004). Further, Zip2 foci are

also distributed with an interference pattern along the coaligned axes of a *zip1*Δ mutant (under conditions where spore formation is reduced from 71% [in wild-type] to 18% in *zip1*Δ [T. Tsubouchi and G.S. Roeder, personal communication], i.e., under mixed "Mode H/Mode L" conditions), and along the coaligned axes of a *msh4*Δ mutant (under "Mode L" conditions). These findings indicate that crossover control, including interference, can occur in the absence of SC, similarly, under both conditions (Fung et al., 2004).

CR interference has previously been studied genetically in *zmm* mutants. Such analyses were always done under Mode L conditions because this is the only condition under which tetrads are formed. In *mer3* Δ, *msh4*Δ, and *zip1*Δ, and *msh5*Δ, the CRs formed do not exhibit detectable interference (Nakagawa and Ogawa, 1999; Novak et al., 2001; Sym and Roeder, 1994; N.H., unpublished data). How can this finding be reconciled with findings from DNA and cytological studies (above)? We suggest that CR interference is, in fact, occurring under Mode L conditions, but is experimentally obscured. This would be because only a few CR-designated DSBs (CR-DSBs) actually mature as CRs (the rest becoming NCRs; below) and interference between these few remaining events will be strongly diluted by the preponderance of noninterfering, ZMM-independent CRs to the point where it is no longer detectable.

CR interference and SC formation occur with similar spatial patterns. Specifically, CR designation sets up ("nucleates") a signal, which then spreads along the homologs in both directions to mediate CR interference. Analogously, SC formation nucleates preferentially at CR-designated sites and spreads in both directions. This relationship contributed to the idea that SC polymerization might mediate CR interference (Introduction), which appears not to be the case (above). Not only does SC polymerization not mediate interference, but in fact, the opposite relationship could pertain, i.e., nucleation and spreading of the CR interference signal directly promotes nucleation and spreading of SC through the corresponding regions. In support of this idea, the interference signal only spreads for a limited distance to either side of its nucleation site, and the same is true of SC formation (for discussion, see Tessé et al., 2003).

A Leptotene/Zygotene Crossover Control Transition

When do CR designation and accompanying interference occur and how are these events coordinated with SC formation? CR designation is signaled by the onset of SEI formation (above). SEI formation is contemporaneous with the onset of SC formation, i.e., leptotene/zygotene (Hunter and Kleckner, 2001). Immediately prior to SC formation, homolog axes are coaligned and linked at a distance of ~400 nm, via axial associations or "bridges" (Figure 8C). These connectors are numerous, apparently representing all recombinational interactions, and contain the RecA recombinases, Dmc1 and Rad51 (reviewed in Hunter and Kleckner, 2001). These features, plus the fact that bridges are DSB-mediated interhomolog connectors, imply that they contain a DSB engaged in a nascent interaction with a homologous partner DNA (Tessé et al., 2003; Hunter and Kleckner, 2001). Most importantly, SC nucleates at a subset of bridge sites and SC nucleation occurs preferentially (or exclusively) at the sites of future CRs (Figure 8C). Together these findings strongly suggest that crossover control and interference are imposed at the bridge stage. Further, at CR-designated bridges, progression to the SEI and nucleation of SC formation would be locally coordinated processes, ultimately yielding an SEI-containing recombination complex surrounded by a patch of SC.

CR designation also sets up interference. Since this effect can operate over very long distances (≥ a chromosome arm), it is attractive to think that the interference signal is transmitted along the homolog axes. We therefore further propose that bridges encountered by the spreading interference signal are designated to become NCRs. NCR designation would include disassembly of the bridge ensemble and would enable the SC to polymerize through such sites. Bridge-associated recombination complexes might already be in a pre-NCR configuration such that those complexes not designated as CRs would proceed to the NCR fate as the default mode. Extension of nucleated SC would also occur in the wake of the spreading interference signal.

The overall effect of these transitions would be to convert bridge-associated DSB ensembles into CR-designated SEI ensembles embedded in and surrounded by continuous SC, a configuration suitable for the next transition along the chiasma pathway, conversion of SEIs to dHJs (Introduction; below).

A ZMM-Mediated Transition at CR-Designated Sites

The *zmm* high temperature phenotype shows that all *zmm* mutants are defective in progression of CR-DSBs to SEIs and in SC formation, which appear to be spatially and temporally coordinate processes. Thus, a simple model would be that all five ZMM proteins (plus Msh4, the partner of Msh5) act together to directly mediate and coordinate the transition of CR-designated DSBs to SEIs plus concomitant nucleation of SC formation, i.e., the conversion of CR-designated bridge ensembles to SEI-recombinosome/SC ensembles (above). This conclusion is supported by the fact that all *zmm* mutants, singles and analyzed doubles, exhibit the same specific defect in final CR levels, which in turn appears to reflect a defect at the DSB to SEI transition. The individual molecular activities and roles for the various ZMMs during this complex series of multiple, mechanistically interdependent processes remain to be determined (below).

The low temperature *zmm* phenotype provides additional information. Under this condition, *zmm* mutants exhibit a modest reduction in CR levels and an increase in NCR levels. One explanation for this phenotype is that CR designation occurs and that CR-DSBs are initially unable to progress, just as at high temperature; they are then finally able to proceed, but with a tendency to lose their fate specification such that a subset mature inappropriately into NCRs. This interpretation is supported by the fact that both CRs and a subset of NCRs arise much later than normal in *zmm* mutants under this condition and by evidence for a subset of late-progressing DSBs in some mutants. It can also explain

the absence of detectable CR interference in this condition (above).

Interestingly, SEIs and dHJs appear to occur abundantly in *zmm* mutants at low temperature. This finding further suggests that ZMM proteins may not be "core biochemical components." For example, they might be part of an auxilliary meiosis-specific machinery that mediates coupling between core biochemical components and underlying chromosome structures. Information could then flow from the recombination ensemble to the structures, e.g., to ensure nucleated SC formation, or, at the next stage, from the SC to the recombination ensemble. Exactly how the biochemical activities such as Mer3 and Msh4/5 would contribute to such coupling is a particularly interesting question. Zip1 would provide a molecular link between the progressing recombination ensembles and SC formation.

Why does recombination occur differently at higher and lower temperatures in *zmm* mutants? As one way to think about this problem we propose that, during wild-type meiosis, a barrier is installed whose role is to impede biochemical progression of CR-designated DSBs until recombinational and structural components are appropriately linked to one another via ZMMs; the resulting ensemble would then mediate an appropriately coupled transition (Figure 8B). At high temperature in *zmm* mutants, the barrier would be intact and the ensuing coordinate transition would not occur due to absence of ZMMs. At low temperature in *zmm* mutants, the barrier would eventually be abrogated such that CR-DSBs can finally progress, but only after a substantial delay and with a tendency to lose fate specification. SC formation would be defective in both cases due to absence of progression at high temperature and due to failure of coupling at low temperature. The sequence of events at sites of CR-designated DSBs and their dependencies on higher temperature and/or ZMM proteins would thus be as follows (Figure 8B): CR-specific core recombination complexes develop independently of ZMM proteins; the progression barrier then develops, promoted either by higher temperature alone and/or lower temperature plus ZMM proteins; finally, ZMM proteins collectively promote the coordinated local SEI-plus-SC nucleation transition. The exact nature of the proposed barrier remains to be determined, but it could involve ATR-mediated, chromosome-based signal transduction (Cha and Kleckner, 2002).

Interestingly, also, non-Zip1 ZMM proteins appear at zygotene/early pachytene and are still present on fully synapsed pachytene chromosomes, in contact with underlying Zip1 within the SC. Thus, it is further possible that the DSB-to-SEI transition is promoted by cytologically undetectable numbers of ZMM protein molecules and that prominent foci arise as a *consequence* of the ZMM-promoted DSB-to-SEI transition, rather than being the *mediators* of that transition. If so, the new, cytologically prominent ZMM ensemble may then mediate the next transition, from SEIs to dHJs (see below).

ZMM proteins may act analogously in other organisms. In *C. elegans* and mouse, *msh4/5* mutants and/or mutants analogous to *zip1*, Rad51 foci occur and persist, implying formation and aberrant progression of DSBs (Edelmann et al., 1999; Colaiacovo et al., 2003). Moreover, as in yeast, mouse *msh4/5* mutations also block SC formation (Edelmann et al., 1999). In *Drosophila*, mutation of the Zip1 analog c(3)G also causes post-DSB defects (Webber et al., 2004).

A Mechanical Model for Crossover Interference

A general model has been described in which mechanical forces arise within chromosomes via programmed expansion of chromatin against constraining features; these forces can do chromosomal work (Kleckner et al., 2004). Mechanical models can readily explain crossover interference because redistribution of mechanical stress or stress relief through a physical system comprises a "communication system" such that occurrence of an event at one position can affect the probability of occurrence of subsequent events at other nearby positions (N.K., unpublished data).

Given that crossover control is imposed at the bridge stage, with the interference signal traveling along the homolog axes (above), we can suggest a specific mechanical model for this process (Figure 8D). Chromatin expansion could result in the development of compression stress (pushing force) along the chromosome axes (N.K., unpublished data). Eventually, such stress causes an axis to buckle. Buckling will tend to occur at the sites of bridges because these represent flaws along the axes. Since stress arises independently along the two homolog axes, buckling will occur first at one end of a particular bridge. This change would place the overlaid recombination complex in a configuration that commits it to becoming a CR and would also promote bridge disassembly, thus releasing the associated recombination complex for further progression. An intrinsic effect of stress-promoted buckling will be local relief of axial compression stress at the affected site. That local stress relief (relaxation) will then spread outwards in both directions, thereby disfavoring subsequent buckling, and thus CR designation events, at adjacent bridges. This effect would explain interference. Spreading axis relaxation could also promote passive elimination of encountered bridges, thus permitting the associated recombination complexes to progress, but only toward the NCR fate. Moreover, buckling and relaxation could directly and/or indirectly promote nucleation and spreading of SC, providing a physical basis for the linkage between CR designation and SC nucleation.

The phenomenon of axis buckling is suggested by cytological images showing that disappearance of bridges is accompanied by a configuration involving bent axes (Figure 8C). Also, in *zip1*Δ and *zip2*Δ mutants, where SC is absent, homolog axes bulge out from discrete "association sites" (e.g., Sym et al., 1993). These associations appear to correspond to sites of (future) CRs and, by the current analysis, the sites of CR-designated DSBs that are failing to progress. This morphology could be a manifestation of CR-correlated axis buckling, which, in the absence of a normal ZMM complex, fails to develop and nucleate SC.

The Role of the SC

The SC does not mediate interference (above). The third transition along the crossover pathway, from SEIs to dHJs, occurs around mid-pachytene in the context of full SCs. Perhaps the SC promotes this transition. A

mechanical model involving stress along the chromosome axes, constrained by the SC, can also explain this transition. Mechanical forces generated by chromatin loop expansion would also tend to cause the SC to twist along its length (N.K., unpublished data). Indeed, twisted SCs are seen routinely (e.g., Figures 1D and 8E). Effects of SC twisting will tend to be focused specifically at sites of SC-associated recombination complexes, which again comprise "weak points" along the structure. SC-associated recombination complexes could then target and transduce axis stresses into local changes. Interestingly, SC twisting is precisely the motion required to bring the axes of the two chromatids involved in recombination into close proximity, thereby promoting their exchange, and ultrastructural evidence is consistent with the idea that axes are exchanged within pachytene SCs (Figure 8E; Moens, 1978). Thus, SC twisting could coordinately govern local changes at both the DNA level (the SEI to dHJ transition) and between chromatid axes (axis exchange). This type of model, in which chromosomal components constrain and transduce mechanical forces, also suggests a rationale for the fact that meiotic prophase involves such prominent structures, not only along the axes but locally at sites of recombination.

Checkpoint Surveillance Monitors Local Events Related to Formation of CRs

At high temperature in *zmm* mutants, both recombination and prophase progression are blocked. Arrest occurs at the end of prophase, prior to SPB separation and spindle formation (e.g., Sym et al., 1993). Arrest prior to meiosis I may be particularly important for yeast because it permits cells to be rescued by return to the mitotic program, e.g., if nutrient conditions permit. In contrast, at low temperature in *zmm* mutants, both recombination and prophase progress efficiently, albeit with a long delay. Importantly, SC formation is absent (in *zip1*Δ) or defective at both temperatures. These patterns imply that the prophase arrest seen at high temperature occurs in response to a block in CR-specific recombination, not a defect in SC formation, thus implying the existence of a late leptotene recombination checkpoint. It remains to be determined whether this checkpoint would also detect a block to NCR events. The nature of the delay observed at low temperature in *zmm* mutants is also unclear. It might reflect an intraprophase surveillance system that senses defective recombination and ensures that other cellular processes remain appropriately coordinated (Lydall et al., 1996).

Further considerations are raised by our results:

- The same mutation can confer either prophase arrest or delayed prophase progression according to the particular conditions of meiosis, not only in yeast (above), but also in other organisms, e.g., male versus female mouse (Hunt and Hassold, 2002). Such differences have previously been attributed to variations in the nature of checkpoint surveillance. The current study shows, at least for *zmm* mutants, that it is the underlying chromosomal processes which differ from one condition to another and which trigger different but appropriate regulatory responses.
- Mutations that alleviate the arrest conferred by *zmm* mutations have been identified and the corresponding proteins have been suggested to be components of checkpoint surveillance mechanisms (Roeder and Bailis, 2000). The current study raises the possibility that at least some of these mutations may be exerting their effects by affecting the recombination process itself rather than its surveillance, e.g., by converting recombination from "Mode H" to "Mode L." Prime candidates for such mutations could include those affecting Dot1/Pch1, Pch2, and Sir2, all of which are chromosomally located and/or affect "chromatin structure" (Roeder and Bailis, 2000; San-Segundo and Roeder, 2000).
- Recombination defects observed in *zmm* mutants are not themselves the consequence of a checkpoint defect. Rather, they are a primary consequence of the absence of locally acting proteins that mediate recombination-related changes.

Temperature Is a Positive Effector of Early Stages of Meiotic Recombination

In wild-type meiosis, both DSBs and SEIs (and thus the leptotene/zygotene transition) occur earlier at 33°C than at 23°C, but thereafter, recombination proceeds similarly at both temperatures. In *zmm* mutants, higher temperature plays a positive role in promoting a key aspect of the leptotene/zygotene transition (above). Other mutant studies suggest that higher temperature may also play a positive role during DSB formation (Kee and Keeney, 2002). Thus, in yeast, higher temperature promotes both earlier and more robust occurrence of the first two steps of meiotic recombination.

Differences between meiosis at higher and lower temperature in yeast appear to be mimicked by those between male and female mouse. In wild-type mouse meiosis, much shorter stretches of Scp3-stained axes are formed prior to onset of SC formation in male as compared to female (F. Baudat and B. deMassy, personal communication), suggesting that onset of the leptotene/zygotene transition is earlier in males. In *zmm*-analogous mutants, meiosis arrests in male while, in female, it "soldiers on" to later stages (Hunt and Hassold, 2002). Meiosis also occurs at different temperatures in the two sexes of mouse, at lower temperature in male, where meiosis occurs in the body periphery, than in female, where it occurs internally (Sod-Moriah et al., 1974). This is the opposite of the relationship predicted, suggesting that the phenomena observed in yeast are not simple "nonspecific" effects of temperature.

Variations in temperature often affect chromosomal processes. Among several possible explanations, an intriguing possibility is that temperature exerts its effects directly by changing the state of the DNA, and thus the chromatin. For example, if chromosomal events are driven by mechanical forces generated by chromatin expansion against constraining features (Kleckner et al., 2004), higher temperature could promote earlier and/or more robust occurrence of chromosomal events by increasing the extent of expansion, and thus the resulting forces. During yeast meiosis, increased stress forces could explain earlier and more robust occurrence of leptotene events as described above.

Experimental Procedures

Strains

All strains are isogenic *MATa/MATα* derivatives of wild-type SK1 and are homozygous for *leu2::hisG, ura3(Pst-Sma), ho::hisG*, heterozygous at the *HIS4LEJ2* locus for either the "standard" *HIS4LEU2* construct or the CR/NCR tester construct (Hunter and Kleckner, 2001; Storlazzi et al., 1995; Figure 1). *zmm* mutant derivatives carry KanMX-marked (Wach et al., 1994) complete deletion mutations. Strains carrying the "standard" construct are: wild-type, NKY3230 (Hunter and Kleckner, 2001); NKY3624, *zip1*Δ; NKY 3625, *zip2*Δ; NKY3626, *zip3*Δ; NKY3627, *msh4*Δ; NKY3628, *msh5*Δ; NKY3629, *mer3*Δ; NKY3630, *zip1*Δ*zip2*Δ; NKY3631, *zip1*Δ*zip3*Δ; NKY3632, *zip2*Δ*zip3*Δ; NKY3633, *msh5*Δ*zip1*Δ. Isogenic *rad50S* (Alani et al., 1990) strains carrying *zip1*Δ, *zip2*Δ, *zip3*Δ, *msh5*Δ, and *mer3*Δ are NKY3634 through NKY3638. Strains containing the CR/NCR *HIS4-LEU2* tester are wild-type, NKY3639; *zip1*Δ; NKY3640, *zip2*Δ; NKY3641, *mer3*Δ; NKY3642, *zip2*Δ*zip3*Δ. BR strains are isogenic to BR2495 (Sym et al., 1993).

Meiotic Timecourses and Analysis of DNA Events

Pregrowth and synchronous meiosis and DNA isolation were as described previously by Bishop et al. (1992) except that YPA medium used for overnight culture preceding transfer to sporulation medium was equilibrated to 30°C prior to inoculation. All experiments were performed under these conditions except those in Figure 5B, in which YPA was at room temperature at the time of inoculation. Under these conditions, all monitored events occur somewhat later than under the standard protocol, but with no basic change in observed patterns, as confirmed by other experiments performed under standard conditions (not shown) as described in Figure 5. For high temperature experiments, cultures were transferred from YPA to sporulation medium pre-equilibrated to 30°C; then, after 2 hr, cultures were shifted to 33°C. For low temperature experiments, cultures were transferred to and then further incubated in sporulation medium pre-equilibrated to 23°C. Sporulation medium contained 0.4% KOAc, 0.02% raffinose, and Antifoam 289 (0.01%, Sigma). Crosslinking of genomic DNA, 1D and 2D gel electrophoresis, and Southern analysis with "Probe A" were as described by Schwacha and Kleckner (1995). For experiments in Figures 3A and 6, crosslinking was omitted. Probes were radiolabeled using Stratagene RmT Random Priming kit. Hybridizing species were quantitated using a Biorad phosphoimager and QuantityOne software. Lifespans and 50% entry and exit times for each DNA stage were calculated as described (Hunter and Kleckner, 2001). The number of DSB events initiated at *HIS4LEU2* was determined by measuring maximum DSB levels in *rad50S* (18.5% and 23.5% at 33°C and 23°C, respectively). The total number of events progressing via SEIs and dHJs was derived from the CRs formed under the respective conditions (18% and 22.5% at 33°C and 23°C, respectively). This corresponds to 14% (SEIs) and 18% (dHJs) at 33°C and 17% (SEIs) and 22.5% (dHJs) at 23°C.

Spore Formation

Aliquots of saturated YPD cultures from a 96-well microtiter dish were "frogged" onto solid sporulation medium (2% K0AC, 0.2% yeast extract, 0.03% "complete mixture" of amino acids and other nutrients [Rose et al., 1990], and 0.06% glucose) and assayed for spore-wall fluorescence (Alani et al., 1990).

Cytological Analysis

Spread nucleoids were prepared and visualized as described (Bishop, 1994) after staining with mouse anti-Zip1 (gift of B. Spyropoulos) at 1/500 and fluorochrome-labeled Alexa 488 goat anti-mouse IgG (Molecular Probes, Oregon) at 1/200. Meiotic divisions were monitored by staining with DAPI (Alani et al., 1990).

Acknowledgments

We thank Oliver Nanassy for unpublished data, Ashwini Jambhekar and Oliver Medvedik for experimental help, and Denise Zickler, Gareth Jones, and Kleckner lab members for discussions. G.V.B. was supported by an EMBO Longterm Fellowship and a Charles A. King Fellowship from the Medical Foundation. N.H. was supported by a Prize Travelling Fellowship from the Wellcome Trust. Research was supported by a grant to N.K. (N.I.H. GM44794).

Received: October 30, 2003
Revised: February 10, 2004
Accepted: March 3, 2004
Published: April 1, 2004

References

Agarwal, S., and Roeder, G.S. (2000). Zip3 provides a link between recombination enzymes and synaptonemal complex proteins. Cell *102*, 245–255.

Alani, E., Padmore, R., and Kleckner, N. (1990). Analysis of wild-type and *rad50* mutants of yeast suggests an intimate relationship between meiotic chromosome synapsis and recombination. Cell *61*, 419–436.

Albini, S.M., and Jones, G.H. (1987). Synaptonemal complex spreading in *Allium cepa* and *A. fistulosum*. I. The initiation and sequence of pairing. Chromosoma *95*, 324–338.

Allers, T., and Lichten, M. (2001). Differential timing and control of noncrossover and crossover recombination during meiosis. Cell *106*, 47–57.

Bishop, D.K. (1994). RecA homologs Dmc1 and Rad51 interact to form multiple nuclear complexes prior to meiotic chromosome synapsis. Cell *79*, 1081–1092.

Bishop, D.K., Park, D., Xu, L., and Kleckner, N. (1992). DMC1: a meiosis-specific yeast homolog of *E. coli* recA required for recombination, synaptonemal complex formation, and cell cycle progression. Cell *69*, 439–456.

Blat, Y., Protacio, R.U., Hunter, N., and Kleckner, N. (2002). Physical and functional interactions among basic chromosome organizational features govern early steps of meiotic chiasma formation. Cell *111*, 791–802.

Byers, B., and Goetsch, L. (1975). Electron microscopic observations on the meiotic karyotype of diploid and tetraploid *Saccharomyces cerevisiae*. Proc. Natl. Acad. Sci. USA *72*, 5056–5060.

Carpenter, A.T. (1987). Gene conversion, recombination nodules, and the initiation of meiotic synapsis. Bioessays *6*, 232–236.

Cha, R.S., and Kleckner, N. (2002). ATR homolog Mec1 promotes fork progression, thus averting breaks in replication slow zones. Science *26*, 602–606.

Chua, P.R., and Roeder, G.S. (1998). Zip2, a meiosis-specific protein required for the initiation of chromosome synapsis. Cell *93*, 349–359.

Colaiacovo, M.P., MacQueen, A.J., Martinez-Perez, E., McDonald, K., Adamo, A., La Volpe, A., and Villeneuve, A.M. (2003). Synaptonemal complex assembly in C. elegans is dispensable for loading strand-exchange proteins but critical for proper completion of recombination. Dev. Cell *5*, 463–474.

Copenhaver, G.P., Housworth, E.A., and Stahl, F.W. (2002). Crossover interference in Arabidopsis. Genetics *160*, 1631–1639.

Darlington, C.D. (1937). Recent Advances in Cytology (Philadelphia, PA: Blakiston).

de los Santos, T., Hunter, N., Lee, C., Larkin, B., Loidl, J., and Hollingsworth, N.M. (2003). The Mus81/Mms4 endonuclease acts independently of double-Holliday junction resolution to promote a distinct subset of crossovers during meiosis in budding yeast. Genetics *164*, 81–94.

Edelmann, W., Cohen, P.E., Kneitz, B., Winand, N., Lia, M., Heyer, J., Kolodner, R., Pollard, J.W., and Kucherlapati, R. (1999). Mammalian MutS homologue 5 is required for chromosome pairing in meiosis. Nat. Genet. *21*, 123–127.

Egel, R. (1978). Synaptonemal complex and crossing-over: structural support or interference? Heredity *41*, 233–237.

Engebrecht, J., Hirsch, J., and Roeder, G.S. (1990). Meiotic gene conversion and crossing over: their relationship to each other and to chromosome synapsis and segregation. Cell *62*, 927–937.

Fung, J.C., Rockmill, B., Odell, M., and Roeder, G.S. (2004). Imposi-

tion of crossover interference through the nonrandom distribution of synapsis initiation complexes. Cell *116*, 795–802.

Henderson, K.A., and Keeney, S. (2004). Tying synaptonemal complex formation to the formation and programmed repair of DNA double-strand breaks. Proc. Natl. Acad. Sci. USA, in press.

Holliday, R. (1964). A mechanism for gene conversion in fungi. Genet. Res. *5*, 282–304.

Hollingsworth, N.M., Ponte, L., and Halsey, C. (1995). MSH5, a novel MutS homolog, facilitates meiotic reciprocal recombination between homologs in *Saccharomyces cerevisiae* but not mismatch repair. Genes Dev. *9*, 1728–1739.

Hunt, P.A., and Hassold, T.J. (2002). Sex matters in meiosis. Science *296*, 2181–2183.

Hunter, N. (2003). Synaptonemal complexities and commonalities. Mol. Cell *12*, 533–535.

Hunter, N., and Kleckner, N. (2001). The single-end invasion: an asymmetric intermediate at the double-strand break to double-Holliday junction transition of meiotic recombination. Cell *106*, 59–70.

Johnson, R.D., and Jasin, M. (2000). Sister chromatid gene conversion is a prominent double-strand break repair pathway in mammalian cells. EMBO J. *19*, 3398–3407.

Jones, G.H. (1984). The control of chiasma distribution. Symp. Soc. Exp. Biol. *38*, 293–320.

Kee, K., and Keeney, S. (2002). Functional interactions between SPO11 and REC102 during initiation of meiotic recombination in Saccharomyces cerevisiae. Genetics *160*, 111–122.

Keeney, S. (2001). Mechanism and control of meiotic recombination initiation. Curr. Top. Dev. Biol. *52*, 1–53.

Kelly, K.O., Dernburg, A.F., Stanfield, G.M., and Villeneuve, A.M. (2000). Caenorhabditis elegans msh-5 is required for both normal and radiation-induced meiotic crossing over but not for completion of meiosis. Genetics *156*, 617–630.

Lichten, M. (2001). Meiotic recombination: breaking the genome to save it. Curr. Biol. *11*, R253–R256.

Lydall, D., Nikolsky, Y., Bishop, D.K., and Weinert, T. (1996). A meiotic recombination checkpoint controlled by mitotic checkpoint genes. Nature *383*, 840–843.

Maguire, M.P. (1966). The relationship of crossing over to chromosome synapsis in a short paracentric inversion. Genetics *53*, 1071–1077.

Moens, P.B. (1978). Lateral element cross connections of the synaptonemal complex and their relationship to chiasmata in rat spermatocytes. Can. J. Genet. Cytol. *20*, 567–579.

Moens, P.B., Kolas, N.K., Tarsounas, M., Marcon, E., Cohen, P.E., and Spyropoulos, B. (2002). The time course and chromosomal localization of recombination-related proteins at meiosis in mouse are compatible with models that can resolve the early DNA-DNA interactions without reciprocal recombination. J. Cell Sci. *115*, 1611–1622.

Nakagawa, T., and Ogawa, H. (1999). The *Saccharomyces cerevisiae* MER3 gene, encoding a novel helicase-like protein, is required for crossover control in meiosis. EMBO J. *18*, 5714–5723.

Novak, J.E., Ross-Macdonald, P.B., and Roeder, G.S. (2001). The budding yeast Msh4 protein functions in chromosome synapsis and the regulation of crossover distribution. Genetics *158*, 1013–1025.

Paques, F., and Haber, J.E. (1999). Multiple pathways of recombination induced by double-strand breaks in *Saccharomyces cerevisiae*. Microbiol. Mol. Biol. Rev. *63*, 349–404.

Rockmill, B., Sym, M., Scherthan, H., and Roeder, G.S. (1995). Roles for two RecA homologs in promoting meiotic chromosome synapsis. Genes Dev. *9*, 2684–2695.

Rockmill, B., Fung, J.C., Branda, S.S., and Roeder, G.S. (2003). The Sgs1 helicase regulates chromosome synapsis and meiotic crossing over. Curr. Biol. *13*, 1954–1962.

Roeder, G.S., and Bailis, J.M. (2000). The pachytene checkpoint. Trends Genet. *16*, 395–403.

Rose, M.D., Winston, F., and Hieter, P. (1990). Methods in Yeast Genetics (Cold Spring Harbor, NY: Cold Spring Harbor Press).

San-Segundo, P.A., and Roeder, G.S. (2000). Role for the silencing protein Dot1 in meiotic checkpoint control. Mol. Biol. Cell *11*, 3601–3615.

Schwacha, A., and Kleckner, N. (1995). Identification of double Holliday junctions as intermediates in meiotic recombination. Cell *83*, 783–791.

Sod-Moriah, U.A., Goldberg, G.M., and Bedrak, E. (1974). Intrascrotal temperature, testicular histology and fertility of heat-acclimatized rats. J. Reprod. Fertil. *37*, 263–268.

Storlazzi, A., Xu, L., Cao, L., and Kleckner, N. (1995). Crossover and noncrossover recombination during meiosis: timing and pathway relationships. Proc. Natl. Acad. Sci. USA *92*, 8512–8516.

Storlazzi, A., Xu, L., Schwacha, A., and Kleckner, N. (1996). Synaptonemal complex (SC) component Zip1 plays a role in meiotic recombination independent of SC polymerization along the chromosomes. Proc. Natl. Acad. Sci. USA *93*, 9043–9048.

Sym, M., and Roeder, G.S. (1994). Crossover interference is abolished in the absence of a synaptonemal complex protein. Cell *79*, 283–292.

Sym, M., Engebrecht, J.A., and Roeder, G.S. (1993). ZIP1 is a synaptonemal complex protein required for meiotic chromosome synapsis. Cell *72*, 365–378.

Tarsounas, M., Morita, T., Pearlman, R.E., and Moens, P.B. (1999). RAD51 and DMC1 form mixed complexes associated with mouse meiotic chromosome cores and synaptonemal complexes. J. Cell Biol. *147*, 207–220.

Tesse, S., Storlazzi, A., Kleckner, N., Gargano, S., and Zickler, D. (2003). Localization and roles of Ski8p protein in *Sordaria* meiosis and delineation of three mechanistically distinct steps of meiotic homolog juxtaposition. Proc. Natl. Acad. Sci. USA *100*, 12865–12870.

von Wettstein, D., Rasmussen, S.W., and Holm, P.B. (1984). The synaptonemal complex in genetic segregation. Annu. Rev. Genet. *18*, 331–413.

Wach, A., Brachat, A., Pohlmann, R., and Philippsen, P. (1994). New heterologous modules for classical or PCR-based gene disruptions in *Saccharomyces cerevisiae*. Yeast *10*, 1793–1808.

Webber, H.A., Howard, L., and Bickel, S.E. (2004). The cohesion protein ORD is required for homolog bias during meiotic recombination. J. Cell Biol. *164*, 819–829.

Zickler, D. (1977). Development of the synaptonemal complex and the "recombination nodules" during meiotic prophase in the seven bivalents of the fungus *Sordaria macrospora* Auersw. Chromosoma *61*, 289–316.

Zickler, D., and Kleckner, N. (1998). The leptotene-zygotene transition of meiosis. Annu. Rev. Genet. *32*, 619–697.

Zickler, D., and Kleckner, N. (1999). Meiotic chromosomes: integrating structure and function. Annu. Rev. Genet. *33*, 603–754.